

Cellular neighborhoods in cancer

Received: 16 April 2025

Accepted: 1 December 2025

Published online: 16 January 2026

 Check for updates

Lichun Ma ^{1,2}✉, Barbara Xiong ^{3,4}, Meng Liu ¹ & Kai Tan ^{5,6,7}✉

The concept of cellular neighborhoods, defined as recurring structures within the tissue with characteristic cell compositions and interactions, has transformed our understanding of the complexity and dynamics of tumor ecosystems. Recent advances in spatial omics and computational modeling have enabled high-resolution mapping of these neighborhoods, providing unprecedented insights into their roles in shaping tumor heterogeneity, evolution and therapeutic responses. Despite these advances, a unified framework for interpreting cellular neighborhoods remains lacking. This Perspective synthesizes emerging concepts and insights, focusing on the definition and classification of cellular neighborhoods in cancer, computational methods for identifying and comparing them, and their clinical relevance.

Just like diverse species in ecological niches, cells and noncellular components coexist and interact in the local microenvironment to form complex ecosystems. This concept has been classically exemplified by the stem cell niche, which supports tissue maintenance, regeneration and repair in systems such as the bone marrow and the gastrointestinal tract^{1,2}. Cellular neighborhoods, defined as recurring spatial structures within the tissue, serve as fundamental units driving the complex and dynamic processes within the tumor microenvironment (TME), such as tumor growth, progression, immune evasion and metastasis.

Spatial exploration of tissue microenvironments has traditionally relied on histology, which has provided foundational insights into cellular morphology, overall tissue architecture and the spatial expression of specific proteins but offers limited resolution of the molecular complexity and cellular interactions underpinning tissue microenvironments. The emergence of spatial omics technologies has paved the way for the deep exploration of tissue microenvironments at high resolution³⁻⁵. Concurrently, a growing suite of computational methods has examined spatial expression patterns, cellular colocalization and discrete cellular neighborhoods⁶⁻⁸.

In this Perspective, we define and classify cellular neighborhoods reported in the literature based on their cellular compositions, functional roles and spatial locations. We also discuss their clinical relevance compared to nonspatial metrics. We provide a comprehensive overview

of computational methods developed to identify cellular neighborhoods from spatial omics data. Lastly, we offer a future perspective on cellular neighborhood research, highlighting key opportunities enabled by emerging spatial omics technologies, the integration of artificial intelligence-driven analytical approaches and the critical importance of experimental validation in establishing the biological relevance of cellular neighborhoods. By integrating these perspectives, this article provides a roadmap for leveraging cellular neighborhoods as a conceptual and analytical framework to advance our understanding of tumor ecosystems, ultimately informing the development of spatially targeted therapeutic strategies.

Definition of cellular neighborhoods

Despite the popular use of cellular neighborhood-based frameworks, consensus on the definition of cellular neighborhoods remains elusive. The terms 'cellular neighborhood', 'niche' and 'spatial domain' are often used interchangeably in the literature, typically referring to an intermediate level of organization between individual cells and whole tissues. Several conceptual definitions of cellular neighborhoods have been proposed in the literature. These definitions include (1) recurring patterns of cell type composition within fixed spatial windows; (2) large histological structures or anatomical compartments, such as tumor cores and immune infiltrates; and (3) tissue regions characterized by

¹Cancer Data Science Laboratory, Center for Cancer Research, National Cancer Institute, Bethesda, MD, USA. ²Liver Cancer Program, Center for Cancer Research, National Cancer Institute, Bethesda, MD, USA. ³Graduate Group in Genomics and Computational Biology, Perelman School of Medicine, University of Pennsylvania, Philadelphia, PA, USA. ⁴Medical Scientist Training Program, Perelman School of Medicine, University of Pennsylvania, Philadelphia, PA, USA. ⁵Department of Pediatrics, Perelman School of Medicine, University of Pennsylvania, Philadelphia, PA, USA. ⁶Division of Oncology and Center for Childhood Cancer Research, Children's Hospital of Philadelphia, Philadelphia, PA, USA. ⁷Center for Single Cell Biology, Children's Hospital of Philadelphia, Philadelphia, PA, USA. ✉e-mail: lichun.ma@nih.gov; tank1@chop.edu

distinct spatial gene expression programs and cell–cell communication patterns. Here, we propose that all cellular neighborhoods share five core defining features: (1) a unique and characteristic cellular composition; (2) spatial restriction within the tissue context; (3) recurrence across tissue regions or samples; (4) enrichment for cell–cell interactions; and (5) a role as a functional unit within the tissue (Fig. 1a). A key axis of variation in existing definitions of cellular neighborhoods relates to their spatial scale. At the local scale, cellular neighborhoods may comprise the immediate microenvironment of a single cell, while at the regional scale, they encompass larger, spatially coherent zones with characteristic cell type compositions or gene expression patterns. Importantly, multiple organizational scales may coexist within the same tissue (Fig. 1b). Many methods for detecting cellular neighborhoods accommodate these varying spatial scales by allowing users to tune the resolution of cellular neighborhood detection. In addition to spatial scale, computational methods differ in the biological features they prioritize, capturing diverse aspects of cellular neighborhoods along the structural–functional axis, ranging from characteristic cell type compositions and spatial expression patterns to cell–cell interactions (Fig. 1c).

Classification of cellular neighborhoods in cancer

Just as histological subtyping has provided standardized frameworks for understanding tumor biology and guiding clinical decision-making, a taxonomy of cellular neighborhoods would enable the systematic characterization of spatial organization across diverse cancer types. Such a framework could capture both conserved and context-specific or tumor type-restricted cellular neighborhoods that reflect unique cellular compositions or interactions. Moreover, a classification system for cellular neighborhoods would provide a foundation for mapping the evolution of these neighborhoods during tumor progression and treatment response or resistance. Ultimately, a standardized cellular neighborhood taxonomy has the potential to transform spatial cancer biology from a largely descriptive field into a predictive and mechanistic discipline, enabling spatially informed precision oncology. Here, we propose the following classification schemes based on the cellular compositions, functional roles and spatial locations of reported cellular neighborhoods in the literature (Fig. 2).

Composition-based classification

One foundational and widely used approach to cellular neighborhood taxonomy is composition-based classification, which defines cellular neighborhoods primarily by the dominant cell types through manual annotation or statistical analysis^{9–12} (Fig. 2). While intuitive and scalable, composition-based classification faces challenges in establishing universal thresholds for what constitutes ‘dominance’. These thresholds can vary across tumor types, tissue contexts and spatial scales. Nonetheless, composition-based classification provides a framework for defining key cellular neighborhood categories and mapping the spatial organization of tumors.

Malignant cell-dominant cellular neighborhoods. Malignant cell-dominant cellular neighborhoods constitute the major structural and functional components of tumors. Based on the abundance of malignant cells, they can be categorized into two groups: malignant-only and malignant–TME interactive neighborhoods. Malignant-only cellular neighborhoods represent densely packed tumor regions with low immunological activity, while malignant–TME interactive neighborhoods are characterized by interactions between malignant cells and TME components such as immune cells, fibroblasts and endothelial cells. These cellular neighborhoods are often involved in immune engagement, stromal remodeling or angiogenic activity, with important roles in tumor progression and immune evasion. Beyond malignant cell abundance, malignant cellular neighborhoods also differ in their cellular states, including epithelial-to-mesenchymal

transition (EMT), cell cycle, interferon response, hypoxia and stress response^{13–16}. These cell states often colocalize with distinct microenvironments, giving rise to subtypes of malignant cell state-associated cellular neighborhoods. For example, in liver cancer, eight distinct malignant cellular neighborhoods were identified based on the spatial organization of cell states, each associated with a unique TME composition¹⁶. In lung cancer, an EMT-associated cellular neighborhood was characterized by spatial interactions among EMT-like malignant cells, myofibroblasts and macrophages¹¹. In ovarian and other cancers, the interferon response-related malignant cell state, marked by high expression of interferon response- and antigen presentation-related genes, preferentially colocalizes with immune cells^{13–17}. Additionally, malignant cells with hypoxia and stress response features, characterized by elevated expression of genes such as *VEGFA*, *HSPA1B* and *ADM*, have been reported across multiple cancer types^{13,16,18–20}. These cellular neighborhoods are often located away from blood vessels and reflect a hypoxia-driven spatial pattern within the TME^{13,19}.

Immune cell-dominant cellular neighborhoods. Immune cell-dominant cellular neighborhoods can be classified into two major subtypes based on their predominant immune cell lineages: lymphoid-dominant and myeloid-dominant. Lymphoid-dominant cellular neighborhoods are primarily composed of T cells and B cells that coordinate adaptive immune responses. A prototypical example is the tertiary lymphoid structure (TLS), characterized by a central zone of CD20⁺ B cells surrounded mainly by CD4⁺ T follicular helper cells. Other immune populations may also be present, including CD8⁺ cytotoxic T cells, T helper 1-polarized CD4⁺ T cells, regulatory T cells, CD68⁺ macrophages and dendritic cells (DCs)^{21,22}. Recent spatial omics studies have identified additional types of lymphoid cellular neighborhoods. For example, lymphonets are spatially organized networks of T cells (particularly TCF1⁺PD-1⁺CD8⁺ T cells) and B cells, which have been identified in lung adenocarcinoma²³. B cell-dominant cellular neighborhoods have also been observed in lung adenocarcinoma, triple-negative breast cancer and acute myeloid leukemia^{10,12,24}.

Myeloid-dominant cellular neighborhoods are characterized by a high abundance of myeloid lineage cells, including macrophages, monocytes, DCs and granulocytes. Each cell type has various subtypes defined by their transcriptional profiles and functional states^{25,26}. This cellular diversity poses a considerable challenge in defining myeloid cellular neighborhoods and understanding their functional roles. As a result, a range of compositionally distinct myeloid cellular neighborhoods has been identified, each associated with context-dependent immune functions. For example, neighborhoods enriched with M1-like macrophages in brain tumors²⁷ and stromal-associated CD68⁺ macrophages in pancreatic ductal adenocarcinoma (PDAC)²⁸ have been linked to antitumor immunity. By contrast, cellular neighborhoods enriched with CSF1R⁺PD-L1⁺ tumor-associated macrophages can suppress immune surveillance by impairing the function of mucosal-associated invariant T cells at the invasive margin of hepatocellular carcinoma (HCC)²⁹. Similarly, environments rich in SPPI⁺/CCL20⁺ macrophages and SPPI⁺/CCL4⁺/IFIT1⁺ neutrophils may form immunosuppressive cellular neighborhoods in liver cancer³⁰. These diverse myeloid-dominant cellular neighborhoods underscore the critical role of cellular composition in shaping their functions. A comprehensive understanding of the subtype diversity and functional states within these cellular neighborhoods is essential for decoding their dynamics in tumor immunity.

Stromal cell-enriched cellular neighborhoods. Stromal cell-enriched cellular neighborhoods, characterized by abundant fibroblasts and endothelial cells, are key regulators of the TME^{31–35}. Four major subtypes of cancer-associated fibroblast (CAF)-enriched cellular neighborhoods have been identified, each with unique cellular compositions, spatial contexts and molecular profiles: CAF–tumor, stromal-enriched,

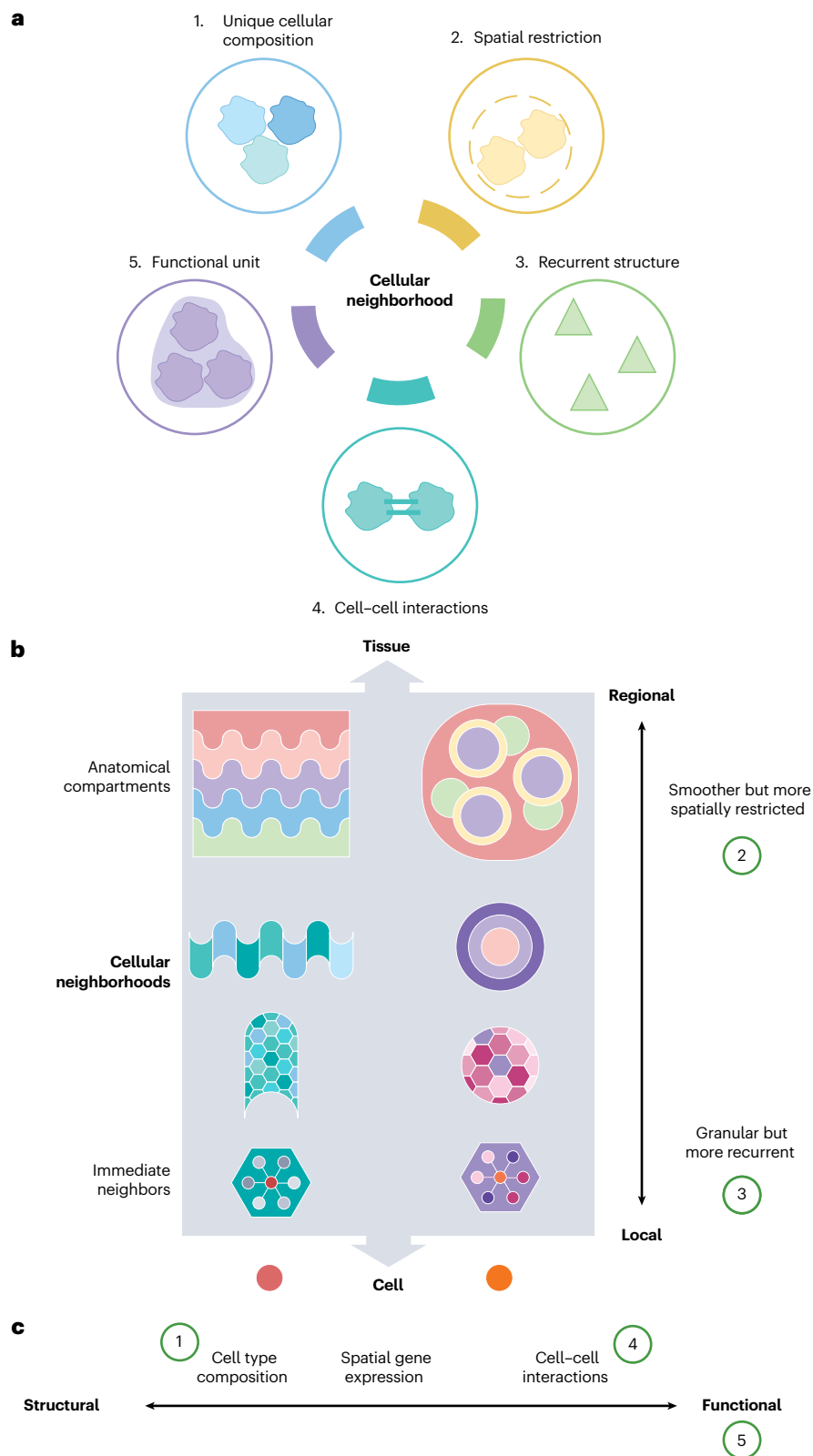


Fig. 1 | Conceptual framework for defining and characterizing cellular neighborhoods in tissues. a, Schematic of five defining features of a cellular neighborhood. **b**, Organizational hierarchy of a tissue. Cellular neighborhoods represent an intermediate spatial unit between individual cells and the tissue as a whole, with a subhierarchy that ranges from granular and recurrent local structures to smoother but more spatially restricted regional domains. Two representative groups of cellular neighborhoods with distinct geometries

(linear versus spherical) are shown in different color tones; within each group, individual units at the next hierarchical level are distinguished by different colors. **c**, Computational approaches for cellular neighborhood identification leverage various features, spanning from structural to functional definitions, including characteristic cell type composition, spatial gene expression patterns and cell-cell interactions.

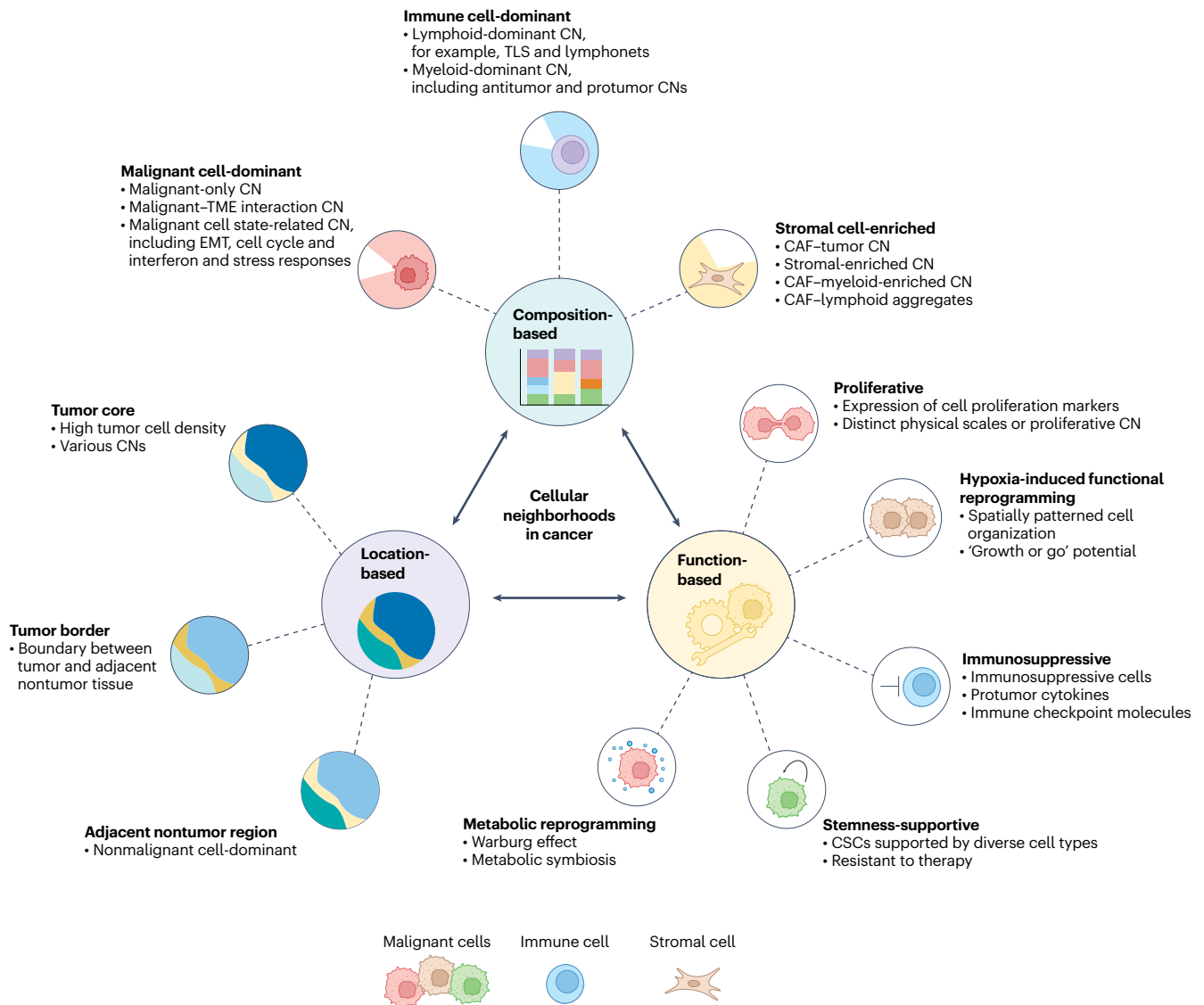


Fig. 2 | Classification of cellular neighborhoods in cancer. Cellular neighborhoods can be classified based on their cellular composition, functional properties and spatial location. The three types of classifications are interconnected. Composition-based classification defines cellular neighborhoods by their dominant cell types, including malignant, immune and stromal cells, while finer subtypes are determined by the presence of specific enriched cell (sub)types. Function-based classification reflects the biological roles of cellular neighborhoods, with proliferative, hypoxia-induced functional

reprogramming, immunosuppressive, stemness-supportive and metabolic reprogramming cellular neighborhoods highlighted here. Spatial location-based classification organizes cellular neighborhoods according to their anatomical context, distinguishing those in the tumor core, tumor border and adjacent nonmalignant tissues. The main features of each type of cellular neighborhood are listed. CN, cellular neighborhood. Figure created in BioRender. Ma, L. (2025) <https://BioRender.com/32d91bu>.

CAF-myeloid-enriched and CAF-lymphoid aggregate cellular neighborhoods³⁶. Each of these CAF-related cellular neighborhoods engages in distinct ligand-receptor interaction networks that shape their functions and influence neighboring cells. For example, cellular interactions through *FGF2-FGFR1*, *TGFBI-TGFBRI* and collagen signaling in CAF-tumor cellular neighborhoods may facilitate ECM remodeling and tumor-stroma crosstalk³⁶⁻³⁸. CAFs within these cellular neighborhoods display elevated expression of collagen and matrix metalloproteinase genes, such as *COL1A1*, *COL3A1*, *COL4A1*, *MMP7* and *MMP14* (ref. 36).

Function-based classification

Although the biological functions of many cellular neighborhoods remain unclear, recent spatial omics studies have identified cellular neighborhoods with specific biological activities. These cellular neighborhoods are characterized by distinct gene expression programs,

enrichment of specific cell types and their spatial context. Here, we highlight cellular neighborhoods that have critical roles in tumor growth and proliferation, tissue remodeling and reprogramming, and immune modulation (Fig. 2).

Proliferative cellular neighborhoods. Excessive cell proliferation is a hallmark of cancer and a key target of many chemotherapeutic agents aimed at eliminating rapidly dividing cells³⁹. Recent studies have revealed that proliferating cells are organized into distinct proliferative cellular neighborhoods rather than being randomly distributed. In PDAC, Ki-67⁺ and Ki-67⁻ tumor or ductal cells form distinct cellular neighborhoods⁴⁰, suggesting that the local environment and neighboring cells may influence the proliferative capacity of cancer cells. Additionally, the size of proliferative cellular neighborhoods can vary, with small cellular neighborhoods (~10–30 μm) representing localized

malignant cell clones that have undergone a few rapid cell divisions, and large cellular neighborhoods (~100–300 μm) reflecting macroenvironmental factors such as hypoxia, nutrient distribution or architectural features of the tumor tissue⁴¹. Further studies are needed to clarify the mechanisms governing the formation and maintenance of these proliferative cellular neighborhoods.

Hypoxia-induced functional reprogramming cellular neighborhoods. Hypoxia is a common feature of most solid tumors, closely linked to tumor aggressiveness, therapeutic resistance and poor patient outcomes^{42,43}. It occurs when malignant cells are distant from oxygen-rich blood vessels, creating gradients of oxygen, nutrients and metabolic wastes⁴⁴. These gradients may, in turn, drive the functional reprogramming of malignant cells and contribute to the formation of spatially organized cellular neighborhoods. For example, in glioblastoma, spatial transcriptome analysis has revealed a layered organization of hypoxia-driven cellular neighborhoods, each with distinct tumor cell states and immune–stromal interactions¹⁹. Hypoxia regulates the ‘growth or go’ potential of tumor cells. As tumors rapidly proliferate, they may shift from the pentose phosphate pathway to glycolysis to survive under low oxygen⁴⁵. This regional hypoxic stress can induce cell cycle arrest and promote the accumulation of copy number variations⁴⁶. A small subset of tumor cells with survival or migratory advantages may escape to normoxic regions, resulting in a reverse-directed trajectory between hypoxia-associated metabolic programming and cellular migration²⁰.

Immunosuppressive cellular neighborhoods. Immunosuppressive cellular neighborhoods are formed through complex interactions among various cell types, with specific immune cell populations—such as regulatory T cells and M2-polarized macrophages—having central roles in orchestrating their immunosuppressive dynamics. A typical immunosuppressive cellular neighborhood is the tumor boundary, which serves as a critical interface where multiple mechanisms converge to support tumor growth and immune evasion^{33,47}. One such mechanism involves a dense, desmoplastic stroma that acts as a physical barrier, limiting immune cell infiltration and disrupting tumor–immune cell interactions^{48,49}. Additionally, malignant and stromal cells produce cytokines and chemokines that recruit immunosuppressive cells, reinforcing a pro-TME⁴⁷. For example, in liver cancer, elevated *CXCL6* expression in malignant cells leads to the recruitment and M2 polarization of macrophages, facilitating the formation of a protumor cellular neighborhood⁵⁰. Furthermore, immunosuppressive cellular neighborhoods are strengthened by the expression of immune checkpoint molecules by both malignant and nonmalignant cells, as observed in melanoma and HCC^{29,47,51}.

Stemness-supportive cellular neighborhoods. A cancer stem cell (CSC) cellular neighborhood represents a supportive microenvironment for CSCs—a subpopulation of tumor cells capable of initiating and sustaining tumor growth, often driving metastasis and relapse^{52–54}. Various cell types, including differentiated malignant cells, immune cells and stromal cells, contribute to the formation of CSC cellular neighborhoods. In glioblastoma, differentiated malignant cells promote the growth of stem cells through BDNF–NTRK2 paracrine signaling, which, in turn, secretes the neuropeptide VGF to support their own survival as well as that of the differentiated malignant cells⁵⁵. Additionally, CAFs and tumor-associated macrophages have been shown to colocalize with CSCs and promote their survival through cytokines such as interleukin-6 (IL-6) and IL-8 (refs. 56–58). In acute myeloid leukemia, nestin⁺ mesenchymal stem cells were found to support the survival of leukemia stem cells⁵⁹.

Metabolic reprogramming cellular neighborhoods. The Warburg effect, in which tumor cells use glycolysis to convert glucose to lactate even in the presence of oxygen, is widespread among tumors. However,

tumor cells may also rely on metabolic interactions with neighboring cells for growth and survival^{20,39,60,61}. For example, in well-oxygenated regions, malignant cells often use lactate from neighboring glycolytic cells as their primary energy source, demonstrating a metabolic symbiosis within the TME^{20,62}. Supporting this model, recent spatial omics studies have revealed a malignant cell-enriched cellular neighborhood exhibiting reduced glycolytic activity and pentose phosphate pathway flux, accompanied by increased glutamine uptake and elevated levels of glutamate^{63–65}. Metabolic symbiosis extends to stromal cells and immune cells, a phenomenon known as the reverse Warburg effect⁶⁶. In PDAC, highly activated metabolic CAFs support tumor metabolism by fueling oxidative phosphorylation⁶⁷. In glioblastoma, lipid-laden macrophages accumulate cholesterol from myelin debris and can then transfer myelin-derived lipids to cancer cells to meet their increased metabolic demands⁶⁸. Tumor cells can also transfer mitochondria to tumor-infiltrating lymphocytes, leading to metabolic dysfunction and impaired antitumor immunity^{69,70}.

Spatial location-based classification

Mapping the locations of cellular neighborhoods within tumors and surrounding tissues can enhance our understanding of tumor architecture. Cellular neighborhoods can be categorized by their spatial locations: tumor core, tumor border and adjacent nonmalignant regions, each representing anatomically distinct compartments with unique cellular and molecular characteristics (Fig. 2)^{11,18,50,71,72}. From a compositional perspective, certain types of cellular neighborhoods tend to localize preferentially to specific compartments. For example, malignant-only cellular neighborhoods are primarily found in the tumor core, while malignant–TME interactive cellular neighborhoods are found in both the tumor core and border^{9,10,16}. In contrast, immune cell-dominant and stromal cell-enriched cellular neighborhoods are observed across various compartments, reflecting their broader roles in the TME^{73,74}. The spatial location of a cellular neighborhood often correlates with its function. Hypoxia-related functional reprogramming cellular neighborhoods are often found in the tumor core, where oxygen deprivation is most pronounced^{19,75}. Immunosuppressive cellular neighborhoods are found in both the tumor core and border. The colocalization of SPPI⁺ macrophages and fibroblasts has been associated with an immunosuppressive environment in these regions^{76,77}. Importantly, the tumor border (that is, the overall boundary between the tumor and adjacent tissue) represents a spatially distinct concept from the tumor invasive front, which specifically refers to the leading edge populated by actively invading malignant cells⁷⁸. Notably, the function of a cellular neighborhood can differ substantially depending on its location. For instance, TLSs within tumors are generally associated with antitumor immunity across cancers, but they are linked to different clinical outcomes in the intratumoral and peritumoral regions in intrahepatic cholangiocarcinoma⁷⁹.

Computational methods for identifying and comparing cellular neighborhoods

Technologies for characterizing the spatial features of the TME have proliferated in recent years. We list key platforms in this fast-developing field in Table 1. These include imaging-based technologies such as CODEX (CO-Detection by indEXing)⁸⁰, CosMx Spatial Molecular Imager and 10x Genomics Xenium, as well as sequencing-based technologies such as 10x Genomics Visium and Stereo-seq⁸¹. CODEX enables the detection of a targeted panel of proteins at cellular resolution⁸⁰. The 10x Genomics Visium platform profiles the whole transcriptome at spot-level resolution, with each spot potentially containing mRNA from multiple cells. CosMx provides whole-transcriptome profiling at single-cell resolution, offering a comprehensive molecular map while preserving spatial context.

The different conceptual definitions of cellular neighborhoods shape computational strategies and influence choices such as the input

Table 1 | Spatial omics profiling methods including the transcriptome, proteome and metabolome

Name	Modality type	Readout type	Resolution	Panel size	Capture area
Visium ¹³⁹	Transcriptomics, limited proteomics	Sequencing	55- μ m spots	Whole transcriptome plus up to 6 proteins	6.5 mm \times 6.5 mm
Visium HD	Transcriptomics	Sequencing	2- μ m spots (recommended to be binned to 8 μ m)	Whole transcriptome	6.5 mm \times 6.5 mm
MERFISH ¹⁴⁰	Transcriptomics, limited proteomics	Imaging	Subcellular	Up to 1,000 genes+ up to 6 proteins	2 cm \times 1.5 cm
Xenium ¹⁴¹	Transcriptomics (simultaneous proteomics in development)	Imaging	Subcellular	Up to 5,000 genes	12 mm \times 24 mm
GeoMx ¹⁴²	Transcriptomics or proteomics	Sequencing	>55- μ m spots	Whole transcriptome	ROI-based
Stereo-seq ⁸¹	Transcriptomics	Sequencing	2- μ m spots	Whole transcriptome	10 mm \times 10 mm, expandable up to 13 cm \times 13 cm
Slide-seqV2 (ref. 143)	Transcriptomics	Sequencing	10- μ m spots	Whole transcriptome	0.3-cm radius
STARmap ¹⁴⁴	Transcriptomics	Imaging	Subcellular	Up to 1,020 genes	Cubic millimeter-scale volumes
Open-ST ¹⁴⁵	Transcriptomics	Sequencing	Subcellular	Whole transcriptome	6.3 mm \times 89 mm (serial sections for virtual 3D)
CosMx ¹⁴⁶	Transcriptomics or proteomics	Imaging	Subcellular	Up 6,200 genes and 68 proteins (separate slide)	15 mm \times 20 mm
CODEX ¹⁴⁷	Proteomics	Imaging	Subcellular	100+ proteins	Whole slide
MIBI-TOF ¹⁴⁸	Proteomics	Imaging+ mass spectrometry	Subcellular	Up to 40 proteins	ROI-based
Imaging mass cytometry ¹⁴⁹	Proteomics	Imaging+ mass spectrometry	1- μ m spots	Up to 40 proteins	ROI-based
t-MALDI-2 MSI ¹⁵⁰	Metabolomics	Imaging+ mass spectrometry	Subcellular	100s metabolites	Square millimeter-scale scan areas

MERFISH, multiplexed error-robust fluorescence in situ hybridization; MIBI-TOF, multiplexed ion beam imaging by time of flight; t-MALDI-2 MSI, transmission-mode MALDI-2 mass spectrometry imaging; ROI, region of interest; 3D, three-dimensional.

data type (cell types versus gene or protein expression), the scale of analysis, the incorporation of spatial priors and the types of biological signals included. The following section outlines key methodological approaches for detecting and comparing cellular neighborhoods from spatial omics data (Table 2).

Clustering-based methods

The most straightforward approaches to cellular neighborhood detection are clustering-based and can be divided into nonspatial and spatial methods. Nonspatial methods are analogous to unsupervised clustering in single-cell data analysis. These methods typically use *k*-means, Louvain, or Leiden clustering on dimension-reduced data or graph embeddings derived from the cell-by-gene matrix. For example, Seurat applies Louvain clustering to a shared nearest-neighbor graph constructed from principal component analysis of expression features⁸². This method is extendable to spot-level spatial transcriptomics data. The spatial versions of these methods explicitly incorporate physical proximity into the detection of cellular neighborhoods. A representative example is the approach by Schürch et al.⁹, in which a *k*-nearest-neighbor (kNN) graph is constructed based on the Euclidean distance between cells within a tissue section. Cells are then clustered using *k*-means based on the frequency of cell types within their ten nearest-neighbor windows. Cells assigned to the same cluster are considered to belong to the same cellular neighborhood⁹. Owing to its simplicity and ease of use, this method has become one of the most widely used approaches in discovery-oriented studies, particularly those using spatial proteomics datasets^{12,27,83}.

Spatially informed clustering-based methods often transform the gene or protein expression matrix or modify the node features of kNN graphs to better capture the spatial context before clustering. For

example, UTAG (Unsupervised discovery of Tissue Architecture with Graphs) uses a ‘message passing’ step to smooth gene expression across neighboring nodes before applying Leiden clustering⁸⁴. BANKSY (Building Aggregates with a Neighborhood Kernel and Spatial Yardstick) augments the gene expression matrix by including the mean expression levels of local kNN neighborhoods and expression gradients from 2kNN neighborhoods⁸⁵. The relative contribution of the original gene expression versus the augmented features is modulated by a lambda parameter, allowing the method to direct the output toward cell type clustering for lower values and cellular neighborhood detection for higher values. Other methods leverage graph-based clustering with additional biological priors. IRIS (Integrative and Reference-Informed tissue Segmentation) performs graph clustering on gene expression features while jointly inferring cell type composition by incorporating a single-cell transcriptomic reference⁸⁶. COVET (Covariance Environment) computes covariance matrices for a cell’s local neighborhood to capture gene expression variation and uses an optimal transport algorithm to determine pairwise distances, resulting in an adjacency matrix that can be clustered to identify cellular neighborhoods⁸⁷.

Probabilistic model-based methods

One subcategory applies the latent Dirichlet allocation (LDA) algorithm, treating neighborhoods as ‘bags-of-cells’, similar to ‘bags-of-words’ in text analysis^{88,89}. Spatial-LDA operates at the cell type level, extending the standard LDA model by using a spatial prior to encourage spatial coherence of neighborhoods⁸⁹. Another subcategory uses Bayesian mixture models with a Potts model-based spatial prior to encourage clustering of neighboring cells. BayesSpace clusters low-dimensional embeddings of gene expression data while using a spatial prior to promote the spatial contiguity of neighboring spots⁹⁰. Building on

Table 2 | Computational methods for identifying and comparing cellular neighborhoods

Name	Method type	Input type	Compatible modalities	Multislice/sample	Description/highlights
Nonspatial clustering (for example, Seurat ⁸²)	Clustering	Expression	All	Yes	Nonspatial <i>k</i> -means, Leiden, or Louvain clustering of cells or spots based on gene expression
Spatial window clustering (for example, Schürch et al. ⁹)	Clustering	Cell type	All	Yes	<i>k</i> -means clustering of kNN cell type frequencies
UTAG ⁸⁴	Clustering	Expression	Imaging-based spatial transcriptomics or proteomics	Yes	Unsupervised graph clustering on gene expression features smoothed with message passing
BANKSY ⁸⁵	Clustering	Expression	All	Yes	Unsupervised graph clustering on low-dimensional embeddings of the augmented gene expression matrix using a spatial kernel, with joint cell type clustering and cellular neighborhood detection
IRIS ⁸⁶	Clustering	Expression	Spot- or imaging-based spatial transcriptomics	Yes	Graph clustering with consideration of cell type-specific single-cell transcriptomic expression profiles and joint modeling of adjacent slices
COVET ⁸⁷	Clustering	Expression	All	No	Uses gene–gene covariance matrices of local niches and optimal transport to define the distance between cells to be dimension-reduced and clustered for TCN characterization
Spatial-LDA ⁸⁹	Probabilistic	Cell type	Imaging-based spatial transcriptomics or proteomics	Yes	Model neighborhoods as ‘bags-of-cells’ using LDA, along with a spatial prior, to sort cells into ‘topics’
BayesSpace ⁹⁰	Probabilistic	Expression	All	No	Bayesian model of a low-dimensional embedding of the gene expression matrix using a spatial prior (Potts model) to ensure clustering of neighboring spots
BASS ⁹¹	Probabilistic	Expression	Imaging-based spatial transcriptomics or proteomics	Yes	Introduces an additional hierarchical modeling structure on top of the Potts model to allow for simultaneous cell type clustering and neighborhood detection
SpaGCN ⁹²	Deep learning	Expression	All	Yes	GCN integrating gene expression, spatial location and histology
GraphST ⁹⁴	Deep learning	Expression	Spot-based spatial transcriptomics	Yes	GNN with self-supervised contrastive learning to minimize the embedding distance between adjacent spots, as well as batch correction for multislice alignment
CellCharter ⁹⁵	Deep learning	Expression	All	Yes	Graph clustering on features aggregated across neighbors, along with variational autoencoders for dimensionality reduction and batch effect removal
CytoCommunity ⁹³	Deep learning	Cell type	All (deconvolution required for spot-based)	Yes, for supervised mode	Graph convolutional neural network using a MinCut-based loss and a classification loss for a supervised mode that generates condition-specific cellular neighborhoods from sample-level labels
SPACE ⁹⁶	Deep learning	Expression	All	No	Graph autoencoder with an attention network to generate low-dimensional cell representations, jointly learning cell types, cellular neighborhoods and characteristic cell–cell interaction networks
GASTON ⁹⁷	Deep learning	Expression	Spot- or imaging-based spatial transcriptomics	No	Topographical map generation through interpretable deep learning, followed by partitioning of constant isodepth contours to convert continuous representations of cellular neighborhoods into discrete ones.
NicheCompass ⁹⁸	Deep learning	Expression	Imaging- or spot-based spatial transcriptomics	Yes	Variational graph autoencoder with consideration of cellular communication and signaling events

All methods are applicable to cancer data. TCN, tissue cellular neighborhood.

BayesSpace, BASS (Bayesian Analytics for Spatial Segmentation) further extends this model hierarchically, enabling simultaneous inference of cell types and cellular neighborhoods⁹¹.

Deep learning-based methods

Another important class of cellular neighborhood detection methods applies deep learning, often using graph neural network

(GNN)-based architectures. Early examples of this category include SpaGCN, which applies graph convolutional networks (GCNs) with edges determined by spatial proximity and node features encoding gene expression⁹². Another method of note is CytoCommunity, whose ‘unsupervised’ mode uses a GCN framework with a MinCut loss function for smoothing neighborhood boundaries⁹³. In addition, CytoCommunity provides a ‘supervised’ mode, which enables

the identification of condition-specific cellular neighborhoods by training on sample-level categorical labels⁹³. Several newer methods in this category have introduced additional features, such as batch correction for multislice and multisample alignment by GraphST and CellCharter^{94,95}. Other methods, such as SPACE (ST data analysis via interaction-aware cell embedding), provide joint cell type clustering with cellular neighborhood detection⁹⁶. While most cellular neighborhood detection methods generate discrete spatial partitions, GASTON (gradient analysis of spatial transcriptomics organization with neural networks) introduces a topography-inspired approach that first learns a one-dimensional continuous 'isodepth' from spatial gene expression gradients, which is subsequently discretized to define cellular neighborhoods⁹⁷. Finally, emerging methods have begun to model cellular neighborhoods by explicitly incorporating cell–cell signaling information. For example, NicheCompass applies a graph variational autoencoder framework that incorporates prior knowledge from ligand–receptor interaction databases to guide the learning of spatial gene programs⁹⁸.

Performance evaluation of cellular neighborhood detection methods

Given the variety of computational strategies and spatial data modalities, practical guidance on method selection and data analysis is crucial for the biology community. A study benchmarked 19 computational methods for cellular neighborhood identification using real and synthetic spatial transcriptomics data, focusing on four key performance metrics: accuracy, stability, generalizability and scalability⁶. This study confirmed that adding spatial location information considerably improves the accuracy of cellular neighborhood identification. However, no single method outperformed all others across every data modality. Most methods demonstrated the best performance on 10x Genomics Visium data but performed poorly on STARmap and Slide-seqV2 data, likely owing to the clearer spatial boundaries in 10x Genomics Visium data and algorithmic bias toward commonly used platforms. Considering all experimental platforms tested, GraphST, BayesSpace, SpaGCN and STAGATE were the most effective and robust methods. GraphST achieved the best overall balance of clustering accuracy, computational efficiency and memory usage, making it the recommended tool. BayesSpace, while accurate, is slower, and STAGATE requires more memory. Notably, the authors found that integrating results from multiple methods often enhances robustness, particularly for challenging datasets such as STARmap and Slide-seqV2. They also emphasized that the default parameter settings in GCN-based tools are not always optimal, and users with programming expertise should experiment with tuning these parameters to achieve improved outcomes.

Methods for comparing cellular neighborhoods

An important question in the field is how to quantitatively characterize changes in cellular neighborhoods across various biological conditions, such as treatment response, disease progression or cancer risk subtypes. This challenge holds broad relevance, akin to the foundational roles of sequence alignment and differential expression analysis in genomics. Current cellular neighborhood detection methods lack direct comparison strategies, causing most studies to rely on indirect assessments, such as differential cell type enrichment within cellular neighborhoods. This approach is only feasible when using detection methods that support multislice or multisample alignment of neighborhood labels. Some recent methods, such as COVET and NicheCompass, offer strategies for mapping local niches around individual cells, with NicheCompass enabling spatial reference mapping of query cells into predefined niche spaces^{87,98}. Similarly, the window-based cellular neighborhood detection method has been extended to map the local niches of a specific cell type—T cells—onto a UMAP (uniform manifold approximation and projection) for visualization⁹⁹.

While probabilistic methods such as Spatial-LDA explicitly model the cell type composition of cellular neighborhoods, methods that capture higher-order spatial structures or recurrent organizational motifs remain limited. An exception is SMORE, a spatial motif discovery tool that operates independently of cellular neighborhood detection by representing spatial graphs through random walks¹⁰⁰. Further development of computational methods for cellular neighborhood comparison and alignment would be highly valuable, enabling the mapping of spatiotemporal trajectories of the TME during treatment or revealing differences in the spatial architecture of tumors across patient subtypes and clinical outcomes.

Clinical implications of cellular neighborhoods

A major challenge in cancer management is the lack of robust biomarkers for predicting patient outcomes and therapeutic responses. Understanding how cellular neighborhoods relate to clinical outcomes could reveal neighborhood-specific vulnerabilities, offering new opportunities to develop therapeutic strategies aimed at disrupting the cellular and molecular wiring within the TME.

Patient prognosis

Growing evidence suggests that cellular neighborhoods are crucial in determining patient prognosis in various cancers. By capturing localized cell interactions, cellular neighborhoods may serve as important biomarkers for patient stratification^{9,49,83,101–104}. Two major cellular neighborhood-based approaches have been explored to link spatial architecture with clinical outcomes. The first involves classifying molecular subtypes based on the composition and structure of all identified cellular neighborhoods. For example, in HCC, spatial interactions between malignant cells and immune cells enabled the stratification of patients into four distinct groups with considerably different survival outcomes, with the most favorable group characterized by enriched interactions with CD8⁺ T cells¹⁰⁵. The second approach focuses on the prognostic relevance of individual cellular neighborhoods. In non-small cell lung cancer, patients with CAFs colocalized with malignant cells had the poorest outcomes, whereas those with CAFs colocalized with T cells and B cells in lymphoid aggregates had the most favorable outcomes³⁶. In HCC, a cellular neighborhood characterized by interactions between PD-L1⁺ M2-like macrophages and transforming growth factor- β (TGF β)-mediated tumor cells was associated with CD8⁺ T cell exhaustion and poor survival in patients with minimal residual disease following chemoembolization⁵¹. Blocking PD-L1 and TGF β restored activated CD8⁺ T cells and eliminated residual tumor cells, highlighting the therapeutic potential of targeting dysfunctional cellular neighborhoods⁵¹.

Treatment response

The success of cancer immunotherapy highlights the importance of the immune landscape's composition and organization as key predictors of treatment responses. Among immune cell-dominant cellular neighborhoods, TLSs are particularly notable and are generally associated with favorable outcomes in various cancers²¹. In patients with non-small cell lung cancer treated with anti-PD-1/PD-L1 antibodies, the presence of mature TLSs, characterized by the co-occurrence of CD20⁺ B cells, CD3⁺ T cells and CD23⁺ follicular DCs, was associated with improved treatment responses and better survival outcomes¹⁰⁶. By contrast, immature TLSs, which lack CD23⁺ follicular DCs, showed no relevant correlation with clinical outcomes¹⁰⁶. In HCC, a cellular neighborhood consisting of mature immunoregulatory DCs, CXCL13⁺ T helper cells and progenitor CD8⁺ T cells was linked to better responses to PD-1 blockade¹⁰⁷. In lung cancer, stem-immunity hubs enriched with stem-like TCF7⁺PD-1⁺CD8⁺ T cells, activated CCR7⁺LAMP3⁺ DCs and CCL19⁺ fibroblasts have been associated with a beneficial response to PD-1 blockade¹⁰¹.

Malignant cell-associated cellular neighborhoods also have an important role in shaping treatment responses. In ovarian cancer, a

malignant cell state characterized by high expression of chemokines, oxidative stress-related genes and antigen presentation molecules colocalized with tumor-infiltrating lymphocytes and was linked to better patient responses to immunotherapy¹⁷. In triple-negative breast cancer, spatial interactions of malignant cells with B cells and GZMB⁺ T cells predicted patient responses to chemotherapy combined with anti-PD-L1 immunotherapy, but not to chemotherapy alone¹⁰⁸, emphasizing the context-dependent clinical relevance of tumor-immune cellular neighborhoods.

Comparison to nonspatial metrics

Nonspatial metrics, such as cell type abundance, gene expression profiles and genetic alterations, provide valuable insights into cancer biology and patient prognosis. However, recent studies suggest that incorporating spatial information, such as cell-cell interactions and neighborhood structures, can considerably improve clinical predictions^{109–112}. In small cell lung cancer, unlike individual immune cell abundance, an MT² cellular neighborhood—defined by a niche of antitumor macrophages, CD8⁺ T cells and natural killer T cells—was linked to better patient outcomes and predicted responses to anti-PD-L1 immunotherapy⁸³. Similarly, in glioblastoma, although the abundance of astrocyte-like malignant cells did not correlate with patient prognosis, their spatial interactions correlated with poor prognosis¹¹³. In contrast, interactions between astrocyte-like cells and other malignant cell states were associated with better prognosis¹¹³. In cutaneous T cell lymphomas, an anti-PD-1 clinical trial found no differences in the frequencies of immune and malignant cells between responders and nonresponders, but close proximity of PD-1⁺CD4⁺ T cells to malignant cells correlated with a better treatment response¹¹⁴. These studies collectively highlight the critical role of spatial information in improving clinical outcome predictions.

Conclusion and future perspectives

In the context of cancer, the concept of cellular neighborhoods provides a powerful lens through which to interrogate the spatial architecture of tumors. Cellular neighborhood-based analyses reveal localized patterns of interaction and signaling that are often obscured in bulk or nonspatial single-cell analyses. This Perspective provides a roadmap for leveraging cellular neighborhoods as a conceptual and analytical framework to advance our understanding of tumor ecosystems, ultimately informing the development of spatially targeted therapeutic strategies.

Looking ahead, as spatial omics technologies continue to scale, the resulting massive high-dimensional datasets provide an ideal substrate for artificial intelligence and foundation models to learn generalizable biological and spatial features that can be further applied to a wide range of tasks. Similar approaches have already transformed single-cell analysis and digital pathology¹¹⁵, enabling data integration, cell type annotation, identification of gene features, prediction of unseen gene perturbations^{116–120}, cancer diagnosis and survival prediction^{121–124}. Growing spatial omics data now open the door for foundation models that can perform cell segmentation, integrate multimodal spatial data measurements (such as spatial proteomics, transcriptomics and metabolomics) and link single-cell profiles with spatial context^{125–128}. Such advances may enable more precise identification and characterization of cellular neighborhoods, ultimately deepening our understanding of their spatial biology.

Parallel efforts have emerged to compile the growing volume of spatial omics datasets into centralized, publicly accessible databases, including STOmicsDB, SODB and SOAR^{129–131}, to support collaborative research. These resources lay the foundation for integrating spatial omics data across diverse tissues, cancer types and disease states into pan-tissue and pan-cancer cellular neighborhood atlases, which may allow for a more rigorous characterization of the taxonomic properties of cellular neighborhoods and how they are conserved or diverge

across cancer types. Ultimately, the curation of gold-standard cellular neighborhoods could provide critical benchmarks for calibrating and validating computational methods for cellular neighborhood detection, addressing a substantial gap in the current spatial omics field, particularly within cancer research.

While cellular neighborhood atlases provide valuable guidance for mechanistic investigations and clinical applications, experimental validation is essential to establish causality. Candidate cellular neighborhoods can be functionally tested through the integration of spatial profiling technologies with genetic perturbation platforms such as Perturb-map, Perturb-FISH and CRISPRmap^{132–134}. Traditional preclinical models, such as xenograft models and genetically engineered mouse models, remain important for probing cellular neighborhood functions but are constrained by species differences and incomplete representation of the human TME^{135,136}. Bioengineering strategies hold potential for the generation of synthetic cellular neighborhoods to model the human-specific TME and investigate cellular neighborhood-specific cell interactions, signaling dynamics and therapeutic vulnerabilities¹³⁷. While tissue-on-a-chip systems have previously been developed to recapitulate multicellular tissue architecture, similar bioengineering platforms could be adapted to reconstruct cellular neighborhoods as defined subecosystems within tissues^{137,138}.

References

- Wilson, A. & Trumpp, A. Bone-marrow haematopoietic-stem-cell niches. *Nat. Rev. Immunol.* **6**, 93–106 (2006).
- Brittan, M. & Wright, N. A. Gastrointestinal stem cells. *J. Pathol.* **197**, 492–509 (2002).
- Bressan, D., Battistoni, G. & Hannon, G. J. The dawn of spatial omics. *Science* **381**, eabq4964 (2023).
- Lewis, S. M. et al. Spatial omics and multiplexed imaging to explore cancer biology. *Nat. Methods* **18**, 997–1012 (2021).
- Park, J. et al. Spatial omics technologies at multimodal and single cell/subcellular level. *Genome Biol.* **23**, 256 (2022).
- Kang, L., Zhang, Q., Qian, F., Liang, J. & Wu, X. Benchmarking computational methods for detecting spatial domains and domain-specific spatially variable genes from spatial transcriptomics data. *Nucleic Acids Res.* **53**, gkaf303 (2025).
- Chen, C., Kim, H. J. & Yang, P. Evaluating spatially variable gene detection methods for spatial transcriptomics data. *Genome Biol.* **25**, 18 (2024).
- Keren, L. et al. A structured tumor-immune microenvironment in triple negative breast cancer revealed by multiplexed ion beam imaging. *Cell* **174**, 1373–1387 (2018).
- Schürch, C. M. et al. Coordinated cellular neighborhoods orchestrate antitumoral immunity at the colorectal cancer invasive front. *Cell* **182**, 1341–1359 (2020).
- Shiao, S. L. et al. Single-cell and spatial profiling identify three response trajectories to pembrolizumab and radiation therapy in triple negative breast cancer. *Cancer Cell* **42**, 70–84 (2024).
- Pentimalli, T. M. et al. High-resolution molecular atlas of a lung tumor in 3D. Preprint at *bioRxiv* <https://doi.org/10.1101/2023.05.10.539644> (2023).
- Bandyopadhyay, S. et al. Mapping the cellular biogeography of human bone marrow niches using single-cell transcriptomics and proteomic imaging. *Cell* **187**, 3120–3140 (2024).
- Barkley, D. et al. Cancer cell states recur across tumor types and form specific interactions with the tumor microenvironment. *Nat. Genet.* **54**, 1192–1201 (2022).
- Pelka, K. et al. Spatially organized multicellular immune hubs in human colorectal cancer. *Cell* **184**, 4734–4752 (2021).
- Gavish, A. et al. Hallmarks of transcriptional intratumour heterogeneity across a thousand tumours. *Nature* **618**, 598–606 (2023).

16. Liu, M. et al. Tumor cell villages define the co-dependency of tumor and microenvironment in liver cancer. Preprint at *bioRxiv* <https://doi.org/10.1101/2025.03.07.642107> (2025).
17. Yeh, C. Y. et al. Mapping spatial organization and genetic cell-state regulators to target immune evasion in ovarian cancer. *Nat. Immunol.* **25**, 1943–1958 (2024).
18. Ren, Y. et al. Spatial transcriptomics reveals niche-specific enrichment and vulnerabilities of radial glial stem-like cells in malignant gliomas. *Nat. Commun.* **14**, 1028 (2023).
19. Greenwald, A. C. et al. Integrative spatial analysis reveals a multi-layered organization of glioblastoma. *Cell* **187**, 2485–2501 (2024).
20. Ravi, V. M. et al. Spatially resolved multi-omics deciphers bidirectional tumor–host interdependence in glioblastoma. *Cancer Cell* **40**, 639–655 (2022).
21. Schumacher, T. N. & Thommen, D. S. Tertiary lymphoid structures in cancer. *Science* **375**, eabf9419 (2022).
22. Sautès-Fridman, C., Petitprez, F., Calderaro, J. & Fridman, W. H. Tertiary lymphoid structures in the era of cancer immunotherapy. *Nat. Rev. Cancer* **19**, 307–325 (2019).
23. Gaglia, G. et al. Lymphocyte networks are dynamic cellular communities in the immunoregulatory landscape of lung adenocarcinoma. *Cancer Cell* **41**, 871–886 (2023).
24. Sorin, M. et al. Single-cell spatial landscapes of the lung tumour immune microenvironment. *Nature* **614**, 548–554 (2023).
25. Cheng, S. et al. A pan-cancer single-cell transcriptional atlas of tumor infiltrating myeloid cells. *Cell* **184**, 792–809 (2021).
26. Ma, R.-Y., Black, A. & Qian, B.-Z. Macrophage diversity in cancer revisited in the era of single-cell omics. *Trends Immunol.* **43**, 546–563 (2022).
27. Karimi, E. et al. Single-cell spatial immune landscapes of primary and metastatic brain tumours. *Nature* **614**, 555–563 (2023).
28. Wattenberg, M. M. et al. Intratumoral cell neighborhoods coordinate outcomes in pancreatic ductal adenocarcinoma. *Gastroenterology* **166**, 1114–1129 (2024).
29. Ruf, B. et al. Tumor-associated macrophages trigger MAIT cell dysfunction at the HCC invasive margin. *Cell* **186**, 3686–3705 (2023).
30. Xue, R. et al. Liver tumour immune microenvironment subtypes and neutrophil heterogeneity. *Nature* **612**, 141–147 (2022).
31. Quail, D. F. & Joyce, J. A. Microenvironmental regulation of tumor progression and metastasis. *Nat. Med.* **19**, 1423–1437 (2013).
32. Lodyga, M. & Hinz, B. TGF- β —a truly transforming growth factor in fibrosis and immunity. *Semin. Cell Dev. Biol.* **101**, 123–139 (2020).
33. Feng, Y. et al. Spatially organized tumor–stroma boundary determines the efficacy of immunotherapy in colorectal cancer patients. *Nat. Commun.* **15**, 10259 (2024).
34. Cremasco, V. et al. FAP delineates heterogeneous and functionally divergent stromal cells in immune-excluded breast tumors. *Cancer Immunol. Res.* **6**, 1472–1485 (2018).
35. Lavie, D., Ben-Shmuel, A., Erez, N. & Scherz-Shouval, R. Cancer-associated fibroblasts in the single-cell era. *Nat. Cancer* **3**, 793–807 (2022).
36. Liu, Y. et al. Conserved spatial subtypes and cellular neighborhoods of cancer-associated fibroblasts revealed by single-cell spatial multi-omics. *Cancer Cell* **43**, 905–924 (2025).
37. Xie, Y. et al. FGF/FGFR signaling in health and disease. *Signal Transduct. Target. Ther.* **5**, 181 (2020).
38. Calon, A., Tauriello, D. V. F. & Battle, E. TGF- β in CAF-mediated tumor growth and metastasis. *Semin. Cancer Biol.* **25**, 15–22 (2014).
39. Hanahan, D. & Weinberg, R. A. Hallmarks of cancer: the next generation. *Cell* **144**, 646–674 (2011).
40. Sussman, J. H. et al. Multiplexed imaging mass cytometry analysis characterizes the vascular niche in pancreatic cancer. *Cancer Res.* **84**, 2364–2376 (2024).
41. Gaglia, G. et al. Temporal and spatial topography of cell proliferation in cancer. *Nat. Cell Biol.* **24**, 316–326 (2022).
42. Majmudar, A. J., Wong, W. J. & Simon, M. C. Hypoxia-inducible factors and the response to hypoxic stress. *Mol. Cell* **40**, 294–309 (2010).
43. Qiu, G.-Z. et al. Reprogramming of the tumor in the hypoxic niche: the emerging concept and associated therapeutic strategies. *Trends Pharmacol. Sci.* **38**, 669–686 (2017).
44. Smith, E. A. & Hodges, H. C. The spatial and genomic hierarchy of tumor ecosystems revealed by single-cell technologies. *Trends Cancer* **5**, 411–425 (2019).
45. Kathagen, A. et al. Hypoxia and oxygenation induce a metabolic switch between pentose phosphate pathway and glycolysis in glioma stem-like cells. *Acta Neuropathol.* **126**, 763–780 (2013).
46. Seim, J. et al. Hypoxia-induced irreversible S-phase arrest involves down-regulation of cyclin A. *Cell Prolif.* **36**, 321–332 (2003).
47. Nirmal, A. J. et al. The spatial landscape of progression and immunoediting in primary melanoma at single-cell resolution. *Cancer Discov.* **12**, 1518–1541 (2022).
48. Zhao, Y. et al. Stromal cells in the tumor microenvironment: accomplices of tumor progression? *Cell Death Dis.* **14**, 587 (2023).
49. Ma, L., Li, C. C. & Wang, X. W. Roles of cellular neighborhoods in hepatocellular carcinoma pathogenesis. *Annu. Rev. Pathol.* **20**, 169–192 (2025).
50. Wu, L. et al. An invasive zone in human liver cancer identified by Stereo-seq promotes hepatocyte–tumor cell crosstalk, local immunosuppression and tumor progression. *Cell Res.* **33**, 585–603 (2023).
51. Lemaitre, L. et al. Spatial analysis reveals targetable macrophage-mediated mechanisms of immune evasion in hepatocellular carcinoma minimal residual disease. *Nat. Cancer* **5**, 1534–1556 (2024).
52. Plaks, V., Kong, N. & Werb, Z. The cancer stem cell niche: how essential is the niche in regulating stemness of tumor cells? *Cell Stem Cell* **16**, 225–238 (2015).
53. Battle, E. & Clevers, H. Cancer stem cells revisited. *Nat. Med.* **23**, 1124–1134 (2017).
54. Prager, B. C., Xie, Q., Bao, S. & Rich, J. N. Cancer stem cells: the architects of the tumor ecosystem. *Cell Stem Cell* **24**, 41–53 (2019).
55. Wang, X. et al. Reciprocal signaling between glioblastoma stem cells and differentiated tumor cells promotes malignant progression. *Cell Stem Cell* **22**, 514–528 (2018).
56. Su, S. et al. CD10⁺GPR77⁺ cancer-associated fibroblasts promote cancer formation and chemoresistance by sustaining cancer stemness. *Cell* **172**, 841–856 (2018).
57. Wan, S. et al. Tumor-associated macrophages produce interleukin 6 and signal via STAT3 to promote expansion of human hepatocellular carcinoma stem cells. *Gastroenterology* **147**, 1393–1404 (2014).
58. Lu, H. et al. A breast cancer stem cell niche supported by juxtacrine signalling from monocytes and macrophages. *Nat. Cell Biol.* **16**, 1105–1117 (2014).
59. Forte, D. et al. Bone marrow mesenchymal stem cells support acute myeloid leukemia bioenergetics and enhance antioxidant defense and escape from chemotherapy. *Cell Metab.* **32**, 829–843 (2020).
60. Semenza, G. L. Tumor metabolism: cancer cells give and take lactate. *J. Clin. Invest.* **118**, 3835–3837 (2008).
61. Lyssiotis, C. A. & Kimmelman, A. C. Metabolic interactions in the tumor microenvironment. *Trends Cell Biol.* **27**, 863–875 (2017).

62. Kennedy, K. M. & Dewhirst, M. W. Tumor metabolism of lactate: the influence and therapeutic potential for MCT and CD147 regulation. *Future Oncol.* **6**, 127–148 (2010).
63. Sun, C. et al. Spatially resolved metabolomics to discover tumor-associated metabolic alterations. *Proc. Natl Acad. Sci. USA* **116**, 52–57 (2019).
64. Smith, B. et al. Addiction to coupling of the Warburg effect with glutamine catabolism in cancer cells. *Cell Rep.* **17**, 821–836 (2016).
65. Khaliq, A. M. et al. Spatial transcriptomic analysis of primary and metastatic pancreatic cancers highlights tumor microenvironmental heterogeneity. *Nat. Genet.* **56**, 2455–2465 (2024).
66. Wilde, L. et al. Metabolic coupling and the Reverse Warburg Effect in cancer: implications for novel biomarker and anticancer agent development. *Semin. Oncol.* **44**, 198–203 (2017).
67. Wang, Y. et al. Single-cell analysis of pancreatic ductal adenocarcinoma identifies a novel fibroblast subtype associated with poor prognosis but better immunotherapy response. *Cell Discov.* **7**, 36 (2021).
68. Kloosterman, D. J. et al. Macrophage-mediated myelin recycling fuels brain cancer malignancy. *Cell* **187**, 5336–5356 (2024).
69. Ikeda, H. et al. Immune evasion through mitochondrial transfer in the tumour microenvironment. *Nature* **638**, 225–236 (2025).
70. Hioki, K. A. et al. The mosquito effect: regulatory and effector T cells acquire cytoplasmic material from tumor cells through intercellular transfer. *Front. Immunol.* **14**, 1272918 (2023).
71. Mo, C.-K. et al. Tumour evolution and microenvironment interactions in 2D and 3D space. *Nature* **634**, 1178–1186 (2024).
72. Wu, R. et al. Comprehensive analysis of spatial architecture in primary liver cancer. *Sci. Adv.* **7**, eabg3750 (2021).
73. Matusiak, M. et al. Spatially segregated macrophage populations predict distinct outcomes in colon cancer. *Cancer Discov.* **14**, 1418–1439 (2024).
74. Shi, Q. et al. Cross-tissue multicellular coordination and its rewiring in cancer. *Nature* **643**, 529–538 (2025).
75. Jahanban-Esfahlan, R., de la Guardia, M., Ahmadi, D. & Yousefi, B. Modulating tumor hypoxia by nanomedicine for effective cancer therapy. *J. Cell. Physiol.* **233**, 2019–2031 (2018).
76. Liu, Y. et al. Identification of a tumour immune barrier in the HCC microenvironment that determines the efficacy of immunotherapy. *J. Hepatol.* **78**, 770–782 (2023).
77. Sathe, A. et al. Colorectal cancer metastases in the liver establish immunosuppressive spatial networking between tumor-associated SPP1⁺ macrophages and fibroblasts. *Clin. Cancer Res.* **29**, 244–260 (2023).
78. Christofori, G. New signals from the invasive front. *Nature* **441**, 444–450 (2006).
79. Ding, G.-Y. et al. Distribution and density of tertiary lymphoid structures predict clinical outcome in intrahepatic cholangiocarcinoma. *J. Hepatol.* **76**, 608–618 (2022).
80. Black, S. et al. CODEX multiplexed tissue imaging with DNA-conjugated antibodies. *Nat. Protoc.* **16**, 3802–3835 (2021).
81. Chen, A. et al. Spatiotemporal transcriptomic atlas of mouse organogenesis using DNA nanoball-patterned arrays. *Cell* **185**, 1777–1792 (2022).
82. Butler, A., Hoffman, P., Smibert, P., Papalexi, E. & Satija, R. Integrating single-cell transcriptomic data across different conditions, technologies, and species. *Nat. Biotechnol.* **36**, 411–420 (2018).
83. Chen, H. et al. Integrative spatial analysis reveals tumor heterogeneity and immune colony niche related to clinical outcomes in small cell lung cancer. *Cancer Cell* **43**, 519–536 (2025).
84. Kim, J. et al. Unsupervised discovery of tissue architecture in multiplexed imaging. *Nat. Methods* **19**, 1653–1661 (2022).
85. Singhal, V. et al. BANKSY unifies cell typing and tissue domain segmentation for scalable spatial omics data analysis. *Nat. Genet.* **56**, 431–441 (2024).
86. Ma, Y. & Zhou, X. Accurate and efficient integrative reference-informed spatial domain detection for spatial transcriptomics. *Nat. Methods* **21**, 1231–1244 (2024).
87. Haviv, D. et al. The covariance environment defines cellular niches for spatial inference. *Nat. Biotechnol.* **43**, 269–280 (2025).
88. Blei, D. M., Ng, A. Y. & Jordan, M. I. Latent Dirichlet allocation. *J. Mach. Learn. Res.* **3**, 993–1022 (2003).
89. Chen, Z., Soifer, I., Hilton, H., Keren, L. & Jojic, V. Modeling multiplexed images with Spatial-LDA reveals novel tissue microenvironments. *J. Comput. Biol.* **27**, 1204–1218 (2020).
90. Zhao, E. et al. Spatial transcriptomics at subspot resolution with BayesSpace. *Nat. Biotechnol.* **39**, 1375–1384 (2021).
91. Li, Z. & Zhou, X. BASS: multi-scale and multi-sample analysis enables accurate cell type clustering and spatial domain detection in spatial transcriptomic studies. *Genome Biol.* **23**, 168 (2022).
92. Hu, J. et al. SpaGCN: integrating gene expression, spatial location and histology to identify spatial domains and spatially variable genes by graph convolutional network. *Nat. Methods* **18**, 1342–1351 (2021).
93. Hu, Y. et al. Unsupervised and supervised discovery of tissue cellular neighborhoods from cell phenotypes. *Nat. Methods* **21**, 267–278 (2024).
94. Long, Y. et al. Spatially informed clustering, integration, and deconvolution of spatial transcriptomics with GraphST. *Nat. Commun.* **14**, 1155 (2023).
95. Varrone, M., Tavernari, D., Santamaria-Martínez, A., Walsh, L. A. & Ciriello, G. CellCharter reveals spatial cell niches associated with tissue remodeling and cell plasticity. *Nat. Genet.* **56**, 74–84 (2024).
96. Li, Y., Zhang, J., Gao, X. & Zhang, Q. C. Tissue module discovery in single-cell-resolution spatial transcriptomics data via cell–cell interaction-aware cell embedding. *Cell Syst.* **15**, 578–592 (2024).
97. Chitra, U. et al. Mapping the topography of spatial gene expression with interpretable deep learning. *Nat. Methods* **22**, 298–309 (2025).
98. Birk, S. et al. Quantitative characterization of cell niches in spatially resolved omics data. *Nat. Genet.* **57**, 897–909 (2025).
99. Hickey, J. W. et al. T cell-mediated curation and restructuring of tumor tissue coordinates an effective immune response. *Cell Rep.* **42**, 113494 (2023).
100. Samadi, Z., Hao, K. & Askary, A. SMORE: spatial motifs reveal patterns in cellular architecture of complex tissues. *Genome Biol.* **26**, 3 (2025).
101. Chen, J. H. et al. Human lung cancer harbors spatially organized stem-immunity hubs associated with response to immunotherapy. *Nat. Immunol.* **25**, 644–658 (2024).
102. Salié, H. et al. Spatial single-cell profiling and neighbourhood analysis reveal the determinants of immune architecture connected to checkpoint inhibitor therapy outcome in hepatocellular carcinoma. *Gut* **74**, 451–466 (2025).
103. Mascharak, S. et al. Desmoplastic stromal signatures predict patient outcomes in pancreatic ductal adenocarcinoma. *Cell Rep. Med.* **4**, 101248 (2023).
104. Qi, J. et al. Single-cell and spatial analysis reveal interaction of FAP⁺ fibroblasts and SPP1⁺ macrophages in colorectal cancer. *Nat. Commun.* **13**, 1742 (2022).
105. Maestri, E. et al. Spatial proximity of tumor–immune interactions predicts patient outcome in hepatocellular carcinoma. *Hepatology* **79**, 768–779 (2024).

106. Peyraud, F. et al. Spatially resolved transcriptomics reveal the determinants of primary resistance to immunotherapy in NSCLC with mature tertiary lymphoid structures. *Cell Rep. Med.* **6**, 101934 (2025).
107. Magen, A. et al. Intratumoral dendritic cell-CD4⁺ T helper cell niches enable CD8⁺ T cell differentiation following PD-1 blockade in hepatocellular carcinoma. *Nat. Med.* **29**, 1389–1399 (2023).
108. Wang, X. Q. et al. Spatial predictors of immunotherapy response in triple-negative breast cancer. *Nature* **621**, 868–876 (2023).
109. Jia, G. et al. Spatial immune scoring system predicts hepatocellular carcinoma recurrence. *Nature* **640**, 1031–1041 (2025).
110. Ali, H. R. et al. Imaging mass cytometry and multiplatform genomics define the phenogenomic landscape of breast cancer. *Nat. Cancer* **1**, 163–175 (2020).
111. Chen, J., Larsson, L., Swarbrick, A. & Lundeberg, J. Spatial landscapes of cancers: insights and opportunities. *Nat. Rev. Clin. Oncol.* **21**, 660–674 (2024).
112. Väyrynen, S. A. et al. Composition, spatial characteristics, and prognostic significance of myeloid cell infiltration in pancreatic cancer. *Clin. Cancer Res.* **27**, 1069–1081 (2021).
113. Zheng, Y., Carrillo-Perez, F., Pizurica, M., Heiland, D. H. & Gevaert, O. Spatial cellular architecture predicts prognosis in glioblastoma. *Nat. Commun.* **14**, 4122 (2023).
114. Phillips, D. et al. Immune cell topography predicts response to PD-1 blockade in cutaneous T cell lymphoma. *Nat. Commun.* **12**, 6726 (2021).
115. Niazi, M. K. K., Parwani, A. V. & Gurcan, M. N. Digital pathology and artificial intelligence. *Lancet Oncol.* **20**, e253–e261 (2019).
116. Wang, X. et al. A pathology foundation model for cancer diagnosis and prognosis prediction. *Nature* **634**, 970–978 (2024).
117. Huang, Z., Bianchi, F., Yuksekogonul, M., Montine, T. J. & Zou, J. A visual-language foundation model for pathology image analysis using medical twitter. *Nat. Med.* **29**, 2307–2316 (2023).
118. Lu, M. Y. et al. A visual-language foundation model for computational pathology. *Nat. Med.* **30**, 863–874 (2024).
119. Yang, Z. et al. A foundation model for generalizable cancer diagnosis and survival prediction from histopathological images. *Nat. Commun.* **16**, 2366 (2025).
120. Hua, S., Yan, F., Shen, T., Ma, L. & Zhang, X. PathoDuet: foundation models for pathological slide analysis of H&E and IHC stains. *Med. Image Anal.* **97**, 103289 (2024).
121. Cui, H. et al. scGPT: toward building a foundation model for single-cell multi-omics using generative AI. *Nat. Methods* **21**, 1470–1480 (2024).
122. Hao, M. et al. Large-scale foundation model on single-cell transcriptomics. *Nat. Methods* **21**, 1481–1491 (2024).
123. Rood, J. E. et al. The Human Cell Atlas from a cell census to a unified foundation model. *Nature* **637**, 1065–1071 (2025).
124. Boiarsky, R. et al. Deeper evaluation of a single-cell foundation model. *Nat. Mach. Intell.* **6**, 1443–1446 (2024).
125. Wang, H. et al. SpatialAgent: an autonomous AI agent for spatial biology. Preprint at *bioRxiv* <https://doi.org/10.1101/2025.04.03.646459> (2025).
126. Tejada-Lapuerta, A. et al. Nicheformer: a foundation model for single-cell and spatial omics. *Nat. Methods* **22**, 2525–2538 (2025).
127. Marks, M. et al. CellSAM: a foundation model for cell segmentation. *Nat. Methods* **22**, 2585–2593 (2025).
128. Wang, C. et al. scGPT-spatial: continual pretraining of single-cell foundation model for spatial transcriptomics. Preprint at *bioRxiv* <https://doi.org/10.1101/2025.02.05.636714> (2025).
129. Xu, Z. et al. STOmicsDB: a comprehensive database for spatial transcriptomics data sharing, analysis and visualization. *Nucleic Acids Res.* **52**, D1053–D1061 (2024).
130. Yuan, Z. et al. SODB facilitates comprehensive exploration of spatial omics data. *Nat. Methods* **20**, 387–399 (2023).
131. Zheng, Y., Chen, Y., Ding, X., Wong, K. H. & Cheung, E. Aquila: a spatial omics database and analysis platform. *Nucleic Acids Res.* **51**, D827–D834 (2023).
132. Dhainaut, M. et al. Spatial CRISPR genomics identifies regulators of the tumor microenvironment. *Cell* **185**, 1223–1239 (2022).
133. Binan, L. et al. Simultaneous CRISPR screening and spatial transcriptomics reveals intracellular, intercellular, and functional transcriptional circuits. Preprint at *bioRxiv* <https://doi.org/10.1101/2023.11.30.569494> (2023).
134. Gu, J. et al. Mapping multimodal phenotypes to perturbations in cells and tissue with CRISPRmap. *Nat. Biotechnol.* **43**, 1101–1115 (2025).
135. Chuprin, J. et al. Humanized mouse models for immuno-oncology research. *Nat. Rev. Clin. Oncol.* **20**, 192–206 (2023).
136. Connolly, K. A., Fitzgerald, B., Damo, M. & Joshi, N. S. Novel mouse models for cancer immunology. *Annu. Rev. Cancer Biol.* **6**, 269–291 (2022).
137. Ingber, D. E. Human organs-on-chips for disease modelling, drug development and personalized medicine. *Nat. Rev. Genet.* **23**, 467–491 (2022).
138. Leung, C. M. et al. A guide to the organ-on-a-chip. *Nat. Rev. Methods Primers* **2**, 33 (2022).
139. Ståhl, P. L. et al. Visualization and analysis of gene expression in tissue sections by spatial transcriptomics. *Science* **353**, 78–82 (2016).
140. Chen, K. H., Boettiger, A. N., Moffitt, J. R., Wang, S. & Zhuang, X. Spatially resolved, highly multiplexed RNA profiling in single cells. *Science* **348**, aaa6090 (2015).
141. Janesick, A. et al. High resolution mapping of the tumor microenvironment using integrated single-cell, spatial and in situ analysis. *Nat. Commun.* **14**, 8353 (2023).
142. Merritt, C. R. et al. Multiplex digital spatial profiling of proteins and RNA in fixed tissue. *Nat. Biotechnol.* **38**, 586–599 (2020).
143. Stickels, R. R. et al. Highly sensitive spatial transcriptomics at near-cellular resolution with Slide-seqV2. *Nat. Biotechnol.* **39**, 313–319 (2021).
144. Wang, X. et al. Three-dimensional intact-tissue sequencing of single-cell transcriptional states. *Science* **361**, eaat5691 (2018).
145. Schott, M. et al. Open-ST: high-resolution spatial transcriptomics in 3D. *Cell* **187**, 3953–3972 (2024).
146. He, S. et al. High-plex imaging of RNA and proteins at subcellular resolution in fixed tissue by spatial molecular imaging. *Nat. Biotechnol.* **40**, 1794–1806 (2022).
147. Goldtsev, Y. et al. Deep profiling of mouse splenic architecture with CODEX multiplexed imaging. *Cell* **174**, 968–981 (2018).
148. Keren, L. et al. MIBI-TOF: a multiplexed imaging platform relates cellular phenotypes and tissue structure. *Sci. Adv.* **5**, eaax5851 (2019).
149. Giesen, C. et al. Highly multiplexed imaging of tumor tissues with subcellular resolution by mass cytometry. *Nat. Methods* **11**, 417–422 (2014).
150. Niehaus, M., Soltwisch, J., Belov, M. E. & Dreisewerd, K. Transmission-mode MALDI-2 mass spectrometry imaging of cells and tissues at subcellular resolution. *Nat. Methods* **16**, 925–931 (2019).

Acknowledgements

This work was supported by grants from the National Institutes of Health (NIH) under award numbers U2C CA233285 and U54HL165442 (K.T.). L.M. was supported by grants (ZIA BC 012079 and ZIA BC 012083) from the Intramural Research Program of the Center for Cancer Research, US National Cancer Institute. B.X. was supported by NIH grant F30CA298606. K.T. holds the Richard and Sheila Sanford Endowed Chair at CHOP. This research was supported in part by the Intramural Research Program of the NIH. The contributions of the NIH authors were made as part of their official duties as NIH federal

employees, are in compliance with agency policy requirements and are considered works of the US government. However, the findings and conclusions presented in this paper are those of the authors and do not necessarily reflect the views of the NIH or the US Department of Health and Human Services.

Competing interests

The authors declare no competing interests.

Additional information

Correspondence should be addressed to Lichun Ma or Kai Tan.

Peer review information *Nature Cancer* thanks Chenfei Wang and the other, anonymous, reviewer(s) for their contribution to the peer review of this work.

Reprints and permissions information is available at www.nature.com/reprints.

Publisher's note Springer Nature remains neutral with regard to jurisdictional claims in published maps and institutional affiliations.

Springer Nature or its licensor (e.g. a society or other partner) holds exclusive rights to this article under a publishing agreement with the author(s) or other rightsholder(s); author self-archiving of the accepted manuscript version of this article is solely governed by the terms of such publishing agreement and applicable law.

© Springer Nature America, Inc 2026